Role of anisotropic interactions in protein crystallization

Xueyu Song
Department of Chemistry, Iowa State University, Ames, Iowa 50011
(Received 19 November 2001; revised manuscript received 26 February 2002; published 22 July 2002)

We have studied a simple model colloidal fluid to assess the role of anisotropic interactions in crystallization process when the interaction potential is short ranged compared with the size of the molecule, which is the case for the effective interaction between protein molecules in aqueous solutions. Using Monte Carlo simulations we have calculated the phase diagrams of soft dumbbell systems with different anisotropic interactions. It is shown that the anisotropic interactions change the phase behavior not only quantitatively but also qualitatively. By exploiting the anisotropic interactions in the crystallization process additional avenues for the search of optimal crystallization conditions are discussed.

DOI: 10.1103/PhysRevE.66.011909 PACS number(s): 87.15.Aa, 05.70.Fh, 64.70.Dv

Many advances in our understanding of biological systems at the molecular level have been made possible through the knowledge of the atomic structure of proteins. However, a crucial step in the determination of the three-dimensional structure by x-ray crystallography is the production of suitable size crystals. This production is a bottleneck for most protein structure determination processes. Experiments clearly indicate that the success of protein crystallization depends sensitively on the physical conditions of the solution [1]. These conditions include temperature, salt concentration, precipitant, pH, and so on. The optimal crystallization condition often lies in a narrow window within a large set of possibilities. Traditional crystallization experiments are largely based on trial and error. It is therefore useful to understand what kind of physical conditions might lead toward the optimal crystallization conditions and why.

A protein solution can be viewed as a colloidal solution since protein molecules are much larger than solvent molecules. Studies [2,3] have shown that not just the strength but also the range of the interactions between protein molecules is crucial for crystallization. It is known that the range of attraction between spherical colloidal particles has a dramatic effect on the appearance of phase diagrams [2–4]. For a sufficiently short-ranged interaction potential, the liquid phase (corresponding to a phase with relatively high protein concentration) will be metastable. Indeed, the experimentally measured phase diagrams of several proteins have such a metastability [2,3].

Recently, the relationship between this metastability and optimal crystallization conditions has been explored by computer simulations [4] and density functional theory calculations [5]. They showed that the activation barrier for the critical nucleus formation near the metastable critical point is much lower than the condition far away from the critical point, therefore possible better crystallization conditions might lie in that region.

However, almost all of such studies are performed for isotropic interaction potentials. When applied to proteins, the basic assumption is that the anisotropy of interacting entities would have little effect on crystallization process, and we may therefore approximate the orientation dependence by an effective isotropic potential. The validity of this assumption can be justified for the phase behaviors of simple liquids such as small molecules, for which their interaction range is comparable to their sizes. Nontrivial effects of anisotropy such as liquid crystal phases appear only for highly anisotropic molecules [6].

The situation is less clear when the interaction range is much shorter than the size of molecules, which is the case for proteins. Several experimental and theoretical evidences on the nontrivial effect of weak anisotropy on thermodynamics and crystallization process have been put forward recently. Sear has shown the importance of the anisotropic attraction to the existence of solid phase for proteins [7]. Lomakin *et al.* have demonstrated that an anisotropic interaction potential model is crucial to describe the experimental phase diagram of γ_{IIIb}-crystallin [8]. Very recently, Yau and Vekilov demonstrated the first experimental observation of a critical nucleus from apoferritin, a quasispherical protein [9]. It was found that the shape of the critical nuclei formed in the nucleation process of apoferritin is slab-like, consisting of a few planar molecular layers, rather than spherical as assumed in classical or neoclassical nucleation theories.

In this paper, a systematic study of the effect of weak anisotropy on crystallization process of molecules with short-ranged interaction is performed. It is shown that anisotropic interactions could be crucial to crystallization process under certain conditions, not only in a quantitative manner but in a qualitative way also. For small molecules such as N_2 whose interaction potential range is long compared to its size, a plastic crystal phase (a phase without orientational order) always forms first under ambient pressures. In this case, a spherical critical nucleus will be the optimal choice since there is no/weak orientational dependence on the surface free energy of a crystal nucleus. In contrast, the effective interaction between protein molecules is short ranged and weak anisotropy can play an important role by modulating the surface free energy's dependence on the orientational order. Hence, a nonspherical critical nucleus may be the optimal choice as demonstrated by a recent experiment [9].

From a practical point of view of protein crystallization, it is critical to produce a protein crystal with orientational order for the determination of high resolution structure. Our studies indicate that the anisotropic interaction also plays an important role in the formation of orientationally ordered crystals.

The anisotropic model we adopted is a simple ''diatomic interaction site model'' fluid (a soft dumbbell model). The

TABLE I. The coexistence reduced densities (ρ_l^* for fluid, ρ_{ps}^* for plastic solid and ρ_{os}^* for ordered solid) and coexistence pressure (p) of hard dumbbells [14] used in the simulation

L^*	ρ_l^*	ρ_{ps}^*	ρ_{os}^*	p
0.3	1.017	1.07		17.45
0.3		1.195	1.262	39.95
0.6	1.146		1.249	37.97

site-site potential is taken as a hard sphere potential with an attractive Yukawa tail (hard sphere Yukawa),

$$u(r)=\begin{cases}\infty, & r\leqslant\sigma,\\ -\epsilon\dfrac{\exp[-\kappa(r-\sigma)/\sigma]}{4r/\sigma} & r>\sigma,\end{cases}$$

where κ determines the attraction range and σ is the diameter of the hard sphere potential. An anisotropy parameter L^* can be defined as L/σ, where L is the bond length of the molecule. With $L^*=0$, the interaction site potential reduces to the isotropic HSY potential. The isotropic HSY potential has been used for studies of phase behaviors as a function of interaction range [13]. The potential becomes more and more short ranged as κ increases, and it was found that the liquid phase becomes metastable near $\kappa\simeq 6$ for $L^*=0.0$. By varying both κ and L^*, it is possible to change the range of interaction and the anisotropy of the potential in a well-controlled manner.

In order to map out the phase diagram of our model system at various anisotropy and interaction ranges we used the Gibbs-Duhem integration method by Kofke [10] given the known hard dumbbell phase diagram to calculate the solid-fluid coexistence. The liquid-vapor coexistence is obtained by Gibbs ensemble method [11].

For different anisotropy parameter L^*, a fairly complete L^* versus density phase diagram for $0\leqslant L^*\leqslant 1$ has previously been obtained by Monte Carlo simulations [14] and density functional theory [15]. For low anisotropy, the dumbbell fluid freezes into the plastic phase, while the fluid coexists with the orientationally ordered phase at higher bond length parameters. The triple point, where the fluid, plastic, and the ordered phases coexist, occurs at $L^*\simeq 0.382$.

For our implementation of the Kofke integration scheme to trace out the liquid-solid coexistence curve, we can write the Clausius-Clapeyron equation as

$$\left(\frac{d\ln\beta P}{d\beta}\right)=-\frac{\Delta e}{\beta P\Delta v}, \tag{1}$$

where $\Delta e=e_{\mathrm{II}}-e_{\mathrm{I}}$ is the difference in molar energy and $\Delta v=v_{\mathrm{II}}-v_{\mathrm{I}}$ is the difference in molar volume between two phases. The integration is initiated from hard dumbbell coexistence data as $\beta\to\infty$. The initial conditions used in this paper are summarized in Table I.

With this starting point the above first-order differential equation can be solved using prediction-correction method by calculating the right side quantity from simulations [10,13]. For the orientationally ordered solid phase we used the constant pressure Monte Carlo implementation but allowing the change in the unit cell shape [16]. Change in the shape of the unit cell is performed by random displacement in all the elements of the matrix that relates the real coordinates to the scaled coordinates in a unit cube. There are 108 particles for the liquid phase and plastic solid phase (fcc lattice as for the hard dumbbell case [14]) and there are 216 particles for the orientationally ordered solid phase initially with the abc closed packing as in the hard dumbbell case. Increasing the number of particles (256 for fluid and plastic solid) does not change our results within the statistical error of our simulation. The potentials in simulations are truncated at half of the simulation box and minimum imagine convention is used in the calculation of the energy of the system. Most of the integration steps in the simulations are $\Delta\beta=0.05$ and a step size $\Delta\beta=0.01$ has been used in some cases to ensure the convergence of the results. The coexistence between the fluid phase and the ordered solid phase in Fig. 4 is obtained by determining the triple point T_2 and corresponding pressure first, and then resulting coexistence densities, pressure and temperature are used to initiate the Gibbs-Duhem integration.

For Gibbs ensemble simulation [11,12], two simulations are carried out in parallel; one of the liquid phase and one of the vapor as in the Kofke's method. The two systems are held at the same temperature and are allowed to exchange volume and particles, but the total volume and total number of particles of the two systems are fixed. This strategy ensures that, at equilibrium, the pressure and the chemical potential of the two systems are the same. All the simulations are performed using 512 particles and the results are converged within the statistical error of our simulation. For large anisotropic parameter ($L^*=0.6$) many more particles' swap attempts are used, but the ratio between the accepted particles' move and the swap move are kept at about 100 to 1.

Using these two methods some of the phase diagrams of our model systems are shown in Figs. 1–4. In Figs. 1 and 3,

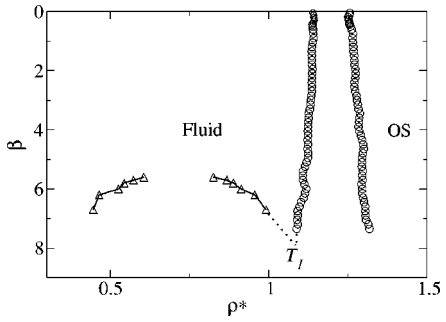

FIG. 1. The phase diagrams of a soft dumbbell system with $\kappa=4.0$ and $L^*=0.6$. β is the reduced inverse temperature and ρ^* is the reduced density [14]. Triangles ($\triangle$) are the coexistence points between the low density and high density fluid phase. Circles ($\bigcirc$) are the coexistence points between the fluid phase and the orientationally ordered solid phase (OS). T_1, which is determined by extrapolation (the dotted lines) of the fluid-fluid coexistence and fluid-solid coexistence, is the traditional triple point involving two fluid phases and the ordered solid phase. The statistical errors are roughly the size of the symbols.

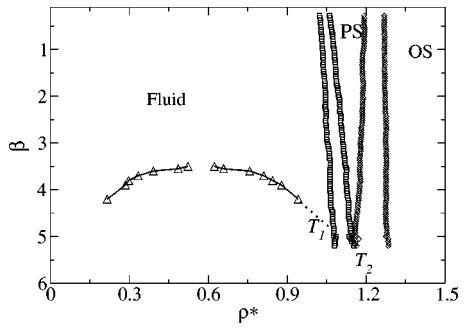

FIG. 2. The phase diagram of a soft dumbbell system with $\kappa = 4.0$ and $L^* = 0.3$. Triangles ($\triangle$) are coexistence points between the low density and high density fluid phases. Squares ($\square$) are the coexistence points between the fluid phase and the plastic solid phase (PS). The diamonds ($\diamond$) are the coexistence densities between the plastic solid phase and the orientationally ordered solid phase. T_1, which is determined by extrapolation of the fluid-fluid coexistence, is the traditional triple point. Another triple point, T_2, involves a fluid phase, a plastic solid phase, and an ordered solid phase. The statistical errors are roughly the size of the symbols.

the phase diagrams are very much like the typical phase diagrams of the corresponding isotropic models [13] except that the solid phase has an orientational order. We did not determine the exact position of the critical points in these phase diagrams due to the slow convergence of Gibbs ensemble simulation. Assuming that the structure of the solid nucleus formed inside a metastable fluid phase closely resembles that of the stable solid phase, it seems reasonable to suppose that for $T < T_1$, orientational ordering inside the nucleus could make the interfacial free energy strongly anisotropic, stabilizing nonspherical morphologies. Therefore, the nucleation process may exploit various nonspherical critical nuclei to lower the activation barrier. At the same time, as in the isotropic case the shorter attraction range ($\kappa = 9$) generated metastable critical point can also be used to facilitate crystallization process [4,5].

In Figs. 2 and 4, the interesting feature in these phase diagrams is the triple point T_2 along the temperature axis. As in strong anisotropic cases ($L^* = 0.6$), relative attraction range determines the stability of the critical point. At the

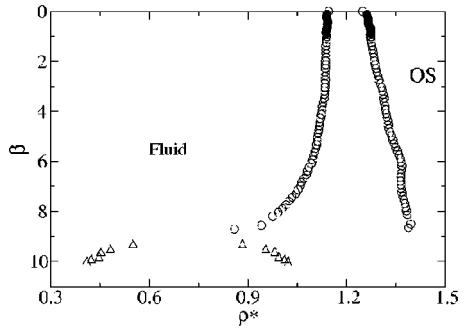

FIG. 3. The phase diagram of a soft dumbbell system with $\kappa = 9.0$ and $L^* = 0.6$. The meaning of the symbols is the same as in Fig. 1. However, the traditional triple point disappears and the critical point becomes metastable in this case.

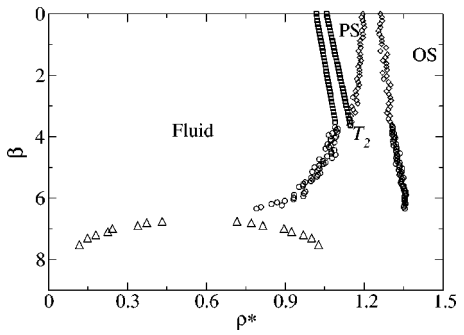

FIG. 4. The phase diagram of a soft dumbbell system with $\kappa = 9.0$ and $L^* = 0.3$. The meaning of the symbols is the same as in Fig. 2. However, the traditional triple point disappears and the second triple point (T_2) survives.

same time we have a competition between two triple points in the weaker anisotropic case. Unlike the simple liquids, however, the location of both triple points in colloidal systems would strongly depend on the parameters of the effective interactions, which in turn depend sensitively on the solution conditions.

It appears that a reasonable proposal can be made about the phase behaviors of these systems based on those calculations. For proteins with weak anisotropy ($L^* < 0.38$ in this model and nonuniform charge distribution on the protein surface could also yield substantial anisotropic interaction as in apoferritin even the geometric anisotropy is small [17]) and $T < T_2$, the plastic phase would be thermodynamically unstable, and the fluid would freeze directly into the orientationally ordered crystal phase. By changing the reduced temperature of the system we can direct the fluid to crystallize into an ordered solid phase. Thus, it seems that it is possible to tune the protein solution conditions such that the protein will crystallize into an orientationally ordered crystal.

To control a protein solution to crystallize into an orientationally ordered crystal form is not just of academic interest, it is crucial also to the high resolution structure determination. For example, some proteins have been crystallized for some time, but their structures have not been solved due to diffusive electron density maps where the orientational disorder in the crystal might be an important source [1,18]. Therefore, as a practical application of this study, phase diagrams of such proteins under experimental conditions may be calculated given the rough geometric shape of the protein determined from other ways such as structural predication method. If it indeed crystallizes into an orientationally disordered phase, by analyzing the distribution of protein molecular orientation, we may be able to help crystallographers to develop a better structural model to explain experimental electron density map. As a matter of fact, in the microtwinning analysis, such a strategy has been employed to find structural models to fit the electron density map of naphthalene dioxygenase [19] and bacteriorhodopsin [20].

The author is grateful to Hyung-June Woo for discussions at the initial stage of this work. Financial support by Petroleum Research Fund, administrated by American Chemical Society is also gratefully acknowledged.

[1] A. McPherson, *The Preparation and Analysis of Protein Crystals* (Wiley, New York, 1982); *Crystallization of Membrane Proteins*, edited by H. Michel (CRC Press, Boca Raton, FL, 1991).
[2] For example, M. Muschol and F. Rosenberger, J. Chem. Phys. **107**, 1953 (1997).
[3] For example, N. Asherie, A. Lomakin, and G.B. Benedek, Phys. Rev. Lett. **77**, 4832 (1996).
[4] P.R. ten Wolde and D. Frenkel, Science **277**, 1975 (1997).
[5] V. Talanquer and D.W. Oxtoby, J. Chem. Phys. **109**, 223 (1998).
[6] P. G. de Gennes and J. Prost, *The Physics of Liquid Crystals*, 2nd ed. (Oxford Science, Oxford, 1993).
[7] R.P. Sear, J. Chem. Phys. **111**, 4800 (1999).
[8] A. Lomakin, N. Asherie, and G.B. Benedek, Proc. Natl. Acad. Sci. U.S.A. **96**, 9465 (1999).
[9] S.T. Yau and P.G. Vekilov, Nature (London) **406**, 494 (2000).
[10] D.A. Kofke, Mol. Phys. **78**, 1331 (1993); D.A. Kofke, Adv. Chem. Phys. **105**, 405 (1999).
[11] A.Z. Panagiotopoulos, Mol. Phys. **61**, 813 (1987).
[12] D. Frenkel and B. Smit, *Understanding Molecular Simulation: From Algorithms to Applications* (Academic Press, San Diego, 1996).
[13] M.H.J. Hagen and D. Frenkel, J. Chem. Phys. **101**, 4093 (1994).
[14] S.J. Singer and R. Mumaugh, J. Chem. Phys. **93**, 1278 (1990); C. Vega, E.P.A. Paras, and P.A. Monson, *ibid.* **97**, 8543 (1992); C. Vega and P.A. Monson, *ibid.* **107**, 2696 (1997).
[15] H.-J. Woo and X. Song, Phys. Rev. E **63**, 051501 (2001).
[16] R. Najafabadi and S. Yip, Scr. Metall. **17**, 1199 (1983); S. Yashonath and C.N.R. Rao, Mol. Phys. **54**, 245 (1985).
[17] X. Song (unpublished).
[18] S. Ramaswamy (private communication).
[19] E. Carredano, B. Kauppi, D. Choudhury, and S. Ramaswamy, Acta Crystallogr., Sect. D: Biol. Crystallogr. **D56**, 313 (2000).
[20] H. Luecke, H.-T. Richter, and J.K. Lanyi, Science **280**, 1934 (1998).